

文章编号: 1007-7294(2024)07-0981-14

三维时域自由面格林函数法的 时域绕射力计算研究

鲁江¹, 张楠¹, 张新曙², 顾民¹

(1. 中国船舶科学研究中心, 江苏无锡 214082; 2. 上海交通大学海洋工程国家重点实验室, 上海 200240)

摘要: 船舶工业CAE软件势流求解器的开发对势流计算方法的可靠性提出要求, 本文针对三维时域面元法开展绕射力计算研究。首先引入三维时域自由面格林函数, 其瞬时项的求解采用Hess & Smith方法, 记忆项的求解采用Beck团队的方法; 其次, 推导出全浪向绕射力脉冲函数法编程所用的数学表达式; 然后, 采用分布源模型求解源强和速度势, 并采用压力直接积分法求出时域绕射力; 最后, 针对Wigley I船型开展绕射力和FK力计算, 并与公开的试验和计算结果进行对比, 验证本文方法的可靠性。本文方法和代码可用于船舶工业CAE软件势流求解器和波浪中船舶非线性失稳运动预报。

关键词: 三维时域面元法; 三维时域格林函数; 绕射力; 船舶CAE自主软件

中图分类号: O353.2 文献标识码: A doi: 10.3969/j.issn.1007-7294.2024.07.002

Diffraction force calculation using three-dimensional time-domain Green function method

LU Jiang¹, ZHANG Nan¹, ZHANG Xin-shu², GU Min¹

(1. China Ship Scientific Research Center, Wuxi 214082, China; 2. State Key Laboratory of Ocean Engineering, Shanghai Jiao Tong University, Shanghai 200240, China)

Abstract: The development of the potential flow solver for the CAE software of a ship requests a reliable method to solve the potential flow. The numerical method of the diffraction force with a three-dimensional time-domain panel method was studied. With a three-dimensional time-domain Green function introduced, its Rankine part was calculated by Hess & Smith's method while its free-surface memory part was calculated by the method of Beck team from the University of Michigan, followed by the derivation of the diffraction impulse function in the mathematical expressions for making the program. Then the source method was used to calculate the source and the diffraction potential, and the diffraction potential force was obtained by integrating the pressure around the floating body. Finally, the diffraction force and Froude-Krylov force were calculated with the Wigley I ship. The verification was carried out by comparing the results with the published experimental and numerical results. The method and the code in this paper are reliable for developing the potential flow solver of the CAE software and predicting the nonlinear stability failure models in waves.

Key words: time-domain panel method; three-dimensional time-domain Green function; diffraction force; CAE software of the ship

收稿日期: 2024-01-15

基金项目: 工信部高技术船舶项目(2017(614))

作者简介: 鲁江(1980-), 男, 博士, 研究员, 通讯作者, E-mail: lujiang1980@aliyun.com;

张楠(1977-), 男, 博士, 研究员。

0 引 言

船舶 CAE 软件是国产船舶行业工业软件体系的重要组成部分,对基于三维时域面元法的势流求解器开发提出了需求。本文在三维时域格林函数计算方法研究^[1]基础上开展三维时域绕射力计算研究。

Finkelstein^[2]提出了线性自由面下的三维时域格林函数;Cummins^[3]和 Ogilvie^[4]首先讨论了非定常运动问题的时域直接求解方法;Wehausen 等^[5]给出了有航速三维时域格林函数积分形式;美国密歇根大学 Beck 团队的 Liapis^[6]、King^[7]、Magee^[8]研究了船舶有航速时的三维时域格林函数法,提出一种三维时域格林函数计算方法,并提出利用脉冲函数和非脉冲函数求解时域绕射力。

Newman^[9-10]提出两套满足不同计算精度的三维时域格林函数计算方法,在此基础上 Bingham^[11]采用三维时域面元法研究了顶浪绕射力求解方法。Osborne^[12]提出了有航速三维时域绕射力和辐射力的 Haskind 关系,研究了随浪绕射力求解方法。Korsmeyer 等^[13]进一步研究了有航速时绕射力的求解方法。Lin 等^[14]对 Newman^[9]提出的三维时域格林函数计算方法做了改进;随后, Lin 等^[15]提出一种满足线性自由面条件的混合源法,以时域 Rankine 源方法为核心,外场匹配时域格林函数来满足辐射条件,以此为基础,美国海军开发了船舶大幅运动评估软件 LAMP^[16],分为 LAMP1 线性版本、LAMP2 弱非线性版本和 LAMP4 全非线性版本,在求解辐射力时同步解出绕射力。

黄德波^[18]导出了三维时域格林函数及其导数的简化计算公式,三维时域格林函数法从此开始在国内得到学者的广泛应用;周正全等^[19]采用黄德波^[18]的三维时域格林函数方法的同时,提出了有航速三维时域绕射力和辐射力的 Haskind 关系;王大云^[20]在采用黄德波的三维时域格林函数方法的基础上,提出了三维水弹性时域分析方法;Clement^[21]、Duan 等^[22]、申亮等^[23]分别推导了三维时域格林函数及其导数满足的四阶微分方程;杨鹏^[24]采用四阶微分方程法计算了三维时域格林函数,采用脉冲函数法计算绕射力;卜淑霞等^[25]、储纪龙等^[26]采用三维时域混合源法求解边界积分方程,在求解辐射力时同步解出绕射力,研究了顶浪和首斜浪参数横摇现象;Chen 等^[27]采用三维时域混合源法构建边界积分方程,并利用泰勒展开边界元法求解边界积分方程,其外域三维时域格林函数及其导数也是采用黄德波^[18]的计算方法。此外,国内针对随浪和尾斜浪中高航速船舶绕射力的计算研究很少。

本文以美国密歇根大学的 Beck 团队的三维时域方法为参照,在文献[1]基础上进一步推导出可直接用于程序开发的全浪向绕射力数学展开表达式,给出求解说明和结果验证,使得三维时域势流求解器的工程开发简单化,促进波浪中操纵性、波浪中快速性、波浪中稳性等学科的发展。

1 数学模型

空间固定坐标系为 $O_0-X_0Y_0Z_0$, 原点位于静水面, X_0 轴为波浪传播方向, Y_0 轴指向左为正, Z_0 轴垂直水面向上为正。参考坐标系为 $O-xyx$, 随着船体以恒定速度 U_0 沿着 x 方向前进, 初始时刻和空间坐标系重合, 不随船体转动而转动。随船坐标系 $O-x'y'z'$ 固定于船体上, 原点和参考坐标系相同, 船体正浮平衡时, 与参考坐标系重合, 随船体的转动而转动。坐标系如图 1 所示。设入射波的浪向角为 β , 船舶航向角为 χ , 则 $\beta = -\chi$ 。

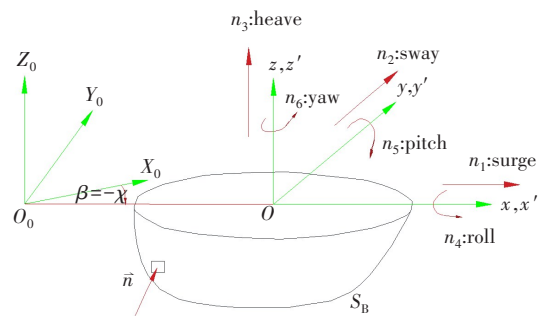


图 1 坐标系
Fig.1 Coordinate system

1.1 绕射力时域直接积分法

在势流理论里,入射波速度势 $\phi_0(x, y, z, t)$ 是已知量,若将坐标 (x, y, z) 标记为 P ,则入射波速度势 $\phi_0(P, t)$ 的表达式为

$$\phi_0(P, t) = \frac{ig}{\omega} e^{k[z - i(x\cos\beta + y\sin\beta)]} e^{i\omega t}, \quad k = \omega^2/g \tag{1}$$

入射波线性化压力表达式为

$$\frac{\partial\phi_0}{\partial t} = \rho g e^{k(z - i(x\cos\beta + y\sin\beta))} e^{i\omega t} \tag{2}$$

任意入射波浪产生的压力采用脉冲函数法可表示为

$$p(P, t) = \int_{-\infty}^{\infty} \hat{p}(P, t - \tau) \zeta(\tau) d\tau \tag{3}$$

式中, $\zeta(\tau)$ 是 τ 时刻参考坐标系下的任意波高, $\hat{p}(P, t)$ 是 t 时刻入射波压力的脉冲函数。

$$\hat{p}(P, t) = F^{-1} \{ \rho g e^{k[z - i(x\cos\beta + y\sin\beta)]} \} = \frac{\rho g}{\pi} \operatorname{Re} \left\{ \int_0^{\infty} e^{k[z - i(x\cos\beta + y\sin\beta)]} e^{i\omega t} d\omega \right\} \tag{4}$$

沿船体湿表面对压力公式(2)进行积分,可得 Froude-Krylov(FK)力在 j 方向的力/力矩表达式:

$$F_{j0} = \iint_{S_B} p(P, t) \cdot n_j dS = \iint_{S_B} \int_{-\infty}^t \hat{p}(P, t - \tau) \zeta(\tau) \cdot n_j d\tau dS = \int_{-\infty}^t \left(\iint_{S_B} \hat{p}(P, t - \tau) \cdot n_j dS \right) \cdot \zeta(\tau) d\tau = \int_{-\infty}^t K_{j0}(t - \tau) \cdot \zeta(\tau) d\tau \tag{5}$$

式中, $K_{j0}(t)$ 为 FK 力脉冲响应函数; $j = 1, 2, \dots, 6$ 分别对应纵荡、横荡、垂荡、横摇、纵摇和首摇 6 个方向。

在势流理论里,入射波速度势 $\phi_0(P, t)$ 是已知量,由式(1)可求出:

$$\nabla\phi_0(P, t) = \begin{bmatrix} \hat{i} \partial\phi_0/\partial x \\ \hat{j} \partial\phi_0/\partial y \\ \hat{k} \partial\phi_0/\partial z \end{bmatrix} = \begin{bmatrix} \hat{i} \cos\beta \\ \hat{j} \sin\beta \\ \hat{k} i \end{bmatrix} \omega e^{k[z - i(x\cos\beta + y\sin\beta)]} e^{i\omega t} \tag{6}$$

任意入射波浪在 x, y, z 方向产生的速度采用脉冲函数法可表示为

$$\nabla\phi_0(P, t) = \int_{-\infty}^t \hat{K}(P, t - \tau) \zeta(\tau) d\tau \tag{7}$$

式中, $\hat{K}(P, t)$ 是入射波速度的脉冲函数,

$$\hat{K}(P, t) = F^{-1} \left\{ \begin{bmatrix} \hat{i} \cos\beta \\ \hat{j} \sin\beta \\ \hat{k} i \end{bmatrix} \omega e^{k[z - i(x\cos\beta + y\sin\beta)]} \right\} = \frac{1}{\pi} \operatorname{Re} \left\{ \begin{bmatrix} \hat{i} \cos\beta \\ \hat{j} \sin\beta \\ \hat{k} i \end{bmatrix} \int_0^{\infty} \omega e^{k[z - i(x\cos\beta + y\sin\beta)]} e^{i\omega t} d\omega \right\} \tag{8}$$

在势流理论里,绕射速度势 $\phi_7(P, t)$ 物面边界条件满足如下表达式:

$$\frac{\partial\phi_7}{\partial n} = -\frac{\partial\phi_0}{\partial n} = -\vec{n} \cdot \nabla\phi_0 = -\vec{n} \cdot \int_{-\infty}^t \hat{K}(P, t - \tau) \zeta(\tau) d\tau \tag{9}$$

把绕射速度势 $\phi_7(P, t)$ 写成脉冲函数表达式:

$$\phi_7(P, t) = \int_{-\infty}^t \hat{\phi}_7(P, t - \tau) \zeta(\tau) d\tau \tag{10}$$

根据式(9),绕射速度势脉冲函数 $\hat{\phi}_7(P, t - \tau)$ 物面边界条件表达式为

$$\frac{\partial\hat{\phi}_7(P, t - \tau)}{\partial n} = -\vec{n} \cdot \vec{K}(P, t - \tau) \tag{11}$$

根据绕射速度势 $\phi_7(P, t)$,沿船体湿表面进行积分,可得绕射力在 j 方向的力/力矩表达式为

$$\begin{aligned}
 F_{j7}(t) &= -\rho \iint_{S_B(t)} \frac{\partial \phi_7}{\partial t} \mathbf{n}_j dS - \rho \iint_{S_B(t)} U_0 \phi_7 \frac{\partial \mathbf{n}_j}{\partial x} dS = -\rho \frac{\partial}{\partial t} \iint_{S_B} \phi_7 \mathbf{n}_j dS + \rho \iint_{S_B} \phi_7 \mathbf{m}_j dS \\
 &= -\rho \frac{\partial}{\partial t} \iint_{S_B} \int_{-\infty}^t \hat{\phi}_7(P, t - \tau) \zeta(\tau) \cdot \mathbf{n}_j d\tau dS + \rho \iint_{S_B} \int_{-\infty}^t d\tau \hat{\phi}_7(P, t - \tau) \zeta(\tau) \cdot \mathbf{m}_j d\tau dS \\
 &= \int_{-\infty}^t \left(-\rho \frac{\partial}{\partial t} \iint_{S_B} \hat{\phi}_7(P, t - \tau) \cdot \mathbf{n}_j dS + \rho \iint_{S_B} \hat{\phi}_7(P, t - \tau) \cdot \mathbf{m}_j dS \right) \zeta(\tau) d\tau \\
 &= \int_{-\infty}^t K_{j7}(t - \tau) \zeta(\tau) d\tau
 \end{aligned} \tag{12}$$

式中, $K_{j7}(t)$ 为绕射力脉冲响应函数; \mathbf{n}_j 为浮体湿表面上在 j 方向矢量, \mathbf{n}_1 是小量, $\mathbf{n}_2, \mathbf{n}_3$ 在 x 方向变化很慢; $(\mathbf{m}_1, \mathbf{m}_2, \dots, \mathbf{m}_6) = (-U_0 \frac{\partial \mathbf{n}_1}{\partial x}, -U_0 \frac{\partial \mathbf{n}_2}{\partial x}, -U_0 \frac{\partial \mathbf{n}_3}{\partial x}, -U_0 \frac{\partial \mathbf{n}_4}{\partial x}, -U_0 \frac{\partial \mathbf{n}_5}{\partial x}, -U_0 \frac{\partial \mathbf{n}_6}{\partial x}) = (0, 0, 0, 0, U_0 \mathbf{n}_3, -U_0 \mathbf{n}_2)$; $\bar{\mathbf{n}}$ 为浮体湿表面上的单位法向矢量, 指向浮体湿表面, 离开流体域。

时域绕射力求解需要求出绕射速度势脉冲函数 $\hat{\phi}_7(P, t - \tau)$, 下面将论述绕射速度势和入射波压力的脉冲函数求解方法。

1.2 三维时域自由面格林函数法

在势流理论里, 时域求解非定常速度势的方法主要有时域自由面格林函数法和时域 Rankine 源法。本文采用三维时域自由面格林函数法, 瞬时项采用 Hess&Smith 方法, 可参见文献[28], 记忆项具体求解方法参见文献[1]。

1.3 间接法求解源密度速度势

同时在物面上布置源和偶极子的方法称为直接法, 仅布置源的方法称为间接法。间接法可以通过边界积分方程得到船体物面的切向速度, 更适合求解考虑瞬时物面的非线性大幅运动问题。间接法求解源密度速度势的论述可参见文献[1]。

1.4 顶浪/首斜浪中绕射速度势和入射波压力脉冲函数求解方法

顶浪/首斜浪中脉冲函数和波高表达式如式(13)~(14)所示(King, 1987)^[7]:

$$\begin{aligned}
 \hat{p}(P, t) &= \frac{\rho g}{\pi} \operatorname{Re} \left\{ \int_0^\infty e^{k[z - i(x \cos \beta + y \sin \beta)]} e^{i\omega_e t} d\omega_e \right\} \\
 \hat{K}(P, t) &= \frac{1}{\pi} \operatorname{Re} \left\{ \begin{bmatrix} \hat{i} \cos \beta \\ \hat{j} \cos \beta \\ \hat{k} \quad i \end{bmatrix} \int_0^\infty \omega e^{k[z - i(x \cos \beta + y \sin \beta)]} e^{i\omega_e t} d\omega_e \right\}
 \end{aligned} \tag{13}$$

$$\zeta(t) = \frac{1}{\pi} \operatorname{Re} \left\{ \int_0^\infty \frac{\bar{\zeta}(\omega)}{1 - \frac{2U_0 \omega \cos \beta}{g}} e^{i\omega_e t} d\omega_e \right\} \tag{14}$$

$$\omega_e = \omega - kU_0 \cos \beta$$

$$d\omega_e = \left(1 - \frac{2\omega}{g} U_0 \cos \beta \right) d\omega \tag{15}$$

把式(15)代入式(13), 可得出下式:

$$\begin{aligned}
 \hat{p}(P, t) &= \frac{\rho g}{\pi} \operatorname{Re} \left\{ \int_0^\infty \left(1 - \frac{2U_0 \cos \beta}{g} \omega \right) e^{\left[\frac{-z}{g} + \frac{i}{g} (x \cos \beta + y \sin \beta + U_0 t \cos \beta) \right] \omega^2} e^{-i\omega t} d\omega \right\} \\
 \hat{K}(P, t) &= \frac{1}{\pi} \operatorname{Re} \left\{ \begin{bmatrix} \hat{i} \cos \beta \\ \hat{j} \cos \beta \\ \hat{k} \quad i \end{bmatrix} \int_0^\infty \left(\omega - \frac{2U_0 \cos \beta}{g} \omega^2 \right) e^{\left[\frac{-z}{g} + \frac{i}{g} (x \cos \beta + y \sin \beta + U_0 t \cos \beta) \right] \omega^2} e^{-i\omega t} d\omega \right\}
 \end{aligned} \tag{16}$$

$$\text{令 } \alpha = -\frac{z}{g} + \frac{i}{g} (x \cos \beta + y \sin \beta + U_0 t \cos \beta), \quad b = -\frac{i t}{2}$$

式(16)的积分部分可写成下面表达式：

$$I_n(\alpha, b) = \int_0^\infty x^n e^{-(\alpha x^2 + 2bx)} dx \tag{17}$$

式(16)可以进一步写成如下表达式：

$$\begin{aligned} \hat{p}(P, t) &= \frac{\rho g}{\pi} \operatorname{Re} \left\{ I_0(\alpha, b) - \frac{2U_0 \cos \beta}{g} I_1(\alpha, b) \right\} \\ \hat{K}(P, t) &= \frac{1}{\pi} \operatorname{Re} \left\{ \begin{bmatrix} \hat{i} \cos \beta \\ \hat{j} \cos \beta \\ \hat{k} \quad i \end{bmatrix} \left(I_1(\alpha, b) - \frac{2U_0 \cos \beta}{g} I_2(\alpha, b) \right) \right\} \end{aligned} \tag{18}$$

通过公式(18)可以看出, 求出 $I_0(\alpha, b)$ 、 $I_1(\alpha, b)$ 、 $I_2(\alpha, b)$ 后, 即可求出顶浪/首斜浪中绕射速度势和入射波压力脉冲函数表达式。

Abramowitz and Stegun^[29]给出下式来计算 I_n ：

$$I_0(\alpha, b) = \int e^{-(\alpha x^2 + 2bx)} dx = \frac{1}{2} \sqrt{\frac{\pi}{\alpha}} e^{\frac{b^2}{\alpha}} \operatorname{erf} \left(\sqrt{\alpha} x + \frac{b}{\sqrt{\alpha}} \right) + \text{constant} \tag{19}$$

$$I_1(\alpha, b) = \int x e^{-(\alpha x^2 + 2bx)} dx = \frac{-b}{2\alpha} \sqrt{\frac{\pi}{\alpha}} e^{\frac{b^2}{\alpha}} \operatorname{erf} \left(\sqrt{\alpha} x + \frac{b}{\sqrt{\alpha}} \right) - \frac{1}{2\alpha} e^{\frac{b^2}{\alpha}} e^{-(\alpha x^2 + 2bx + \frac{b^2}{\alpha})} \tag{20}$$

$$\begin{aligned} I_2(\alpha, b) = \int x^2 e^{-(\alpha x^2 + 2bx)} dx &= \frac{1}{4\alpha} \sqrt{\frac{\pi}{\alpha}} e^{\frac{b^2}{\alpha}} \operatorname{erf} \left(\sqrt{\alpha} x + \frac{b}{\sqrt{\alpha}} \right) + \frac{b^2}{2\alpha^2} \sqrt{\frac{\pi}{\alpha}} e^{\frac{b^2}{\alpha}} \operatorname{erf} \left(\sqrt{\alpha} x + \frac{b}{\sqrt{\alpha}} \right) - \\ &\quad \frac{1}{2} \left(\frac{x}{\alpha} - \frac{b}{\alpha^2} \right) e^{\frac{b^2}{\alpha}} e^{-(\alpha x^2 + 2bx + \frac{b^2}{\alpha})} \end{aligned} \tag{21}$$

$$\lim_{z \rightarrow \infty} \operatorname{erf}(z) = 1 \quad \text{for } |\arg(z)| < \frac{\pi}{4} \tag{22}$$

顶浪/首斜浪中 $I_0(\alpha, b)$ 、 $I_1(\alpha, b)$ 、 $I_2(\alpha, b)$ 的表达式如下：

$$\begin{aligned} I_0 &= \int_0^\infty e^{-(\alpha x^2 + 2bx)} dx = \frac{1}{2} \sqrt{\frac{\pi}{\alpha}} e^{b^2/\alpha} - \frac{1}{2} \sqrt{\frac{\pi}{\alpha}} e^{b^2/\alpha} \operatorname{erf} \left(\frac{b}{\sqrt{\alpha}} \right) = \frac{1}{2} \sqrt{\frac{\pi}{\alpha}} e^{b^2/\alpha} \left(1 - \operatorname{erf} \left(\frac{b}{\sqrt{\alpha}} \right) \right) \\ I_1 &= \int_0^\infty x e^{-(\alpha x^2 + 2bx)} dx = -\frac{b}{2\alpha} \sqrt{\frac{\pi}{\alpha}} e^{b^2/\alpha} + \frac{b}{2\alpha} \sqrt{\frac{\pi}{\alpha}} e^{b^2/\alpha} \operatorname{erf} \left(\frac{b}{\sqrt{\alpha}} \right) + \frac{1}{2\alpha} = -\frac{b}{2\alpha} \sqrt{\frac{\pi}{\alpha}} e^{b^2/\alpha} \left(1 - \operatorname{erf} \left(\frac{b}{\sqrt{\alpha}} \right) \right) + \frac{1}{2\alpha} \tag{23} \\ I_2 &= \int_0^\infty x^2 e^{-(\alpha x^2 + 2bx)} dx = \sqrt{\frac{\pi}{\alpha}} \left(\frac{1}{4\alpha} + \frac{b^2}{2\alpha^2} \right) e^{b^2/\alpha} \left(1 - \operatorname{erf} \left(\frac{b}{\sqrt{\alpha}} \right) \right) - \frac{b}{2\alpha^2} \end{aligned}$$

根据误差函数定义 (Abramowitz and Stegun^[29]),

$$\operatorname{erfc}(z) = 1 - \operatorname{erf}(z), \quad w(z) = e^{-z^2} \operatorname{erfc}(-iz) \tag{24}$$

式(23)可以进一步写成下述表达式：

$$I_0(\alpha, b) = \frac{1}{2} \sqrt{\frac{\pi}{\alpha}} w \left(\frac{i b}{\sqrt{\alpha}} \right), \quad I_1(\alpha, b) = -\frac{b}{\alpha} I_0 + \frac{1}{2\alpha}, \quad I_2(\alpha, b) = -\frac{b}{\alpha} I_1 + \frac{1}{2\alpha} I_0 \tag{25}$$

1.5 随浪/尾斜浪中绕射速度势和入射波压力脉冲函数求解方法

在随浪/尾斜浪中, 同一遭遇频率存在三个入射波长, 脉冲函数和波高按照入射波频率范围分成3部分, King^[7]给出了公式(26)、(27)和(28)：

$$\omega_1 = \frac{g}{2U_0 \cos \beta} \left(1 - \sqrt{1 - \frac{4U_0 \cos \beta}{g} \omega_e} \right) \quad \left(0 < \omega_e < \frac{g}{4U_0 \cos \beta} \right)$$

$$\begin{aligned} \omega_2 &= \frac{g}{2U_0 \cos \beta} \left(1 + \sqrt{1 - \frac{4U_0 \cos \beta}{g} \omega_e} \right) \quad (0 < \omega_e < \frac{g}{4U_0 \cos \beta}) \\ \omega_3 &= \frac{g}{2U_0 \cos \beta} \left(1 + \sqrt{1 + \frac{4U_0 \cos \beta}{g} \omega_e} \right) \quad (0 < \omega_e < \infty) \\ k_m &= \frac{\omega_m^2}{g} \quad m = 1, 2, 3 \end{aligned} \tag{26}$$

$$\begin{aligned} \hat{p}^{(\omega_m)}(P, t) &= \frac{\rho g}{\pi} \operatorname{Re} \left\{ \int_0^{\frac{g}{4U_0 \cos \beta}} e^{k_m [z - i(x \cos \beta + y \sin \beta)]} e^{i\omega_e t} d\omega_e \right\} \quad m = 1, 2 \\ &= \frac{\rho g}{\pi} \operatorname{Re} \left\{ \int_0^\infty e^{k_m [z + i(x \cos \beta + y \sin \beta)]} e^{i\omega_e t} d\omega_e \right\} \quad m = 3 \\ \hat{K}^{(\omega_m)}(P, t) &= \frac{1}{\pi} \operatorname{Re} \left\{ \begin{bmatrix} \hat{i} \cos \beta \\ \hat{j} \cos \beta \\ \hat{k} i \end{bmatrix} \int_0^{\frac{g}{4U_0 \cos \beta}} \omega_m e^{k_m [z - i(x \cos \beta + y \sin \beta)]} e^{i\omega_e t} d\omega_e \right\} \quad m = 1, 2 \\ &= \frac{1}{\pi} \operatorname{Re} \left\{ \begin{bmatrix} \hat{i} \cos \beta \\ \hat{j} \cos \beta \\ \hat{k} i \end{bmatrix} \int_0^\infty \omega_m e^{k_m [z + i(x \cos \beta + y \sin \beta)]} e^{i\omega_e t} d\omega_e \right\} \quad m = 3 \end{aligned} \tag{27}$$

$$\begin{aligned} \zeta^{(\omega_m)}(t) &= \frac{1}{\pi} \operatorname{Re} \left\{ \int_0^{\frac{g}{4U_0 \cos \beta}} \frac{\bar{\zeta}(\omega_m)}{1 - \frac{2U_0 \omega_m \cos \beta}{g}} e^{i\omega_e t} d\omega_e \right\} \quad m = 1, 2 \\ &= \frac{1}{\pi} \operatorname{Re} \left\{ \int_0^\infty \frac{\bar{\zeta}(\omega_m)}{1 - \frac{2U_0 \omega_m \cos \beta}{g}} e^{i\omega_e t} d\omega_e \right\} \quad m = 3 \end{aligned} \tag{28}$$

由式(26)可以得到

$$\begin{aligned} \omega_e &= \omega_1 - \omega_1^2 \frac{U_0 \cos \beta}{g}, \quad d\omega_e = 1 - \frac{2U_0 \cos \beta}{g} \omega_1 \quad (0 < \omega_1 < \frac{g}{2U_0 \cos \beta}) \\ \omega_e &= \omega_2 - \omega_2^2 \frac{U_0 \cos \beta}{g}, \quad d\omega_e = 1 - \frac{2U_0 \cos \beta}{g} \omega_2 \quad (\frac{g}{U_0 \cos \beta} > \omega_2 > \frac{g}{2U_0 \cos \beta}) \\ \omega_e &= -\omega_3 + \omega_3^2 \frac{U_0 \cos \beta}{g}, \quad d\omega_e = -(1 - \frac{2U_0 \cos \beta}{g} \omega_3) \quad (\frac{g}{U_0 \cos \beta} \leq \omega_3 < \infty) \end{aligned} \tag{29}$$

把式(29)代入式(27), 可得出式(30)~(34):

$$\hat{K}^{(\omega_1)}(P, t) = \frac{1}{\pi} \operatorname{Re} \left\{ \begin{bmatrix} \hat{i} \cos \beta \\ \hat{j} \cos \beta \\ \hat{k} i \end{bmatrix} \int_0^{\frac{g}{2U_0 \cos \beta}} \left(1 - \frac{2U_0 \cos \beta}{g} \omega_1 \right) \omega_1 e^{k_1 [z - i(x \cos \beta + y \sin \beta + U_0 t \cos \beta)]} e^{i\omega_1 t} d\omega_1 \right\} \tag{30}$$

$$\hat{K}^{(\omega_2)}(P, t) = -\frac{1}{\pi} \operatorname{Re} \left\{ \begin{bmatrix} \hat{i} \cos \beta \\ \hat{j} \cos \beta \\ \hat{k} i \end{bmatrix} \int_{\frac{g}{2U_0 \cos \beta}}^{\frac{g}{U_0 \cos \beta}} \left(1 - \frac{2U_0 \cos \beta}{g} \omega_2 \right) \omega_2 e^{k_2 [z - i(x \cos \beta + y \sin \beta + U_0 t \cos \beta)]} e^{i\omega_2 t} d\omega_2 \right\} \tag{31}$$

$$\hat{K}^{(\omega_3)}(P, t) = -\frac{1}{\pi} \operatorname{Re} \left\{ \begin{bmatrix} \hat{i} \cos \beta \\ \hat{j} \cos \beta \\ \hat{k} i \end{bmatrix} \int_{\frac{g}{U_0 \cos \beta}}^{\infty} \left(1 - \frac{2U_0 \cos \beta}{g} \omega_3 \right) \omega_3 e^{k[z - i(x \cos \beta + y \sin \beta + U_0 t \cos \beta)]} e^{i \omega_3 t} d\omega_3 \right\} \quad (32)$$

$$\hat{p}^{(\omega_1)}(P, t) = \frac{\rho g}{\pi} \operatorname{Re} \left\{ \int_0^{\frac{g}{2U_0 \cos \beta}} \left(1 - \frac{2U_0 \cos \beta}{g} \omega_1 \right) \omega_1 e^{k_1[z - i(x \cos \beta + y \sin \beta + U_0 t \cos \beta)]} e^{i \omega_1 t} d\omega_1 \right\}$$

$$\hat{p}^{(\omega_2)}(P, t) = -\frac{\rho g}{\pi} \operatorname{Re} \left\{ \int_{\frac{g}{2U_0 \cos \beta}}^{\frac{g}{U_0 \cos \beta}} \left(1 - \frac{2U_0 \cos \beta}{g} \omega_2 \right) \omega_2 e^{k_2[z - i(x \cos \beta + y \sin \beta + U_0 t \cos \beta)]} e^{i \omega_2 t} d\omega_2 \right\} \quad (33)$$

$$\hat{p}^{(\omega_3)}(P, t) = -\frac{\rho g}{\pi} \operatorname{Re} \left\{ \int_{\frac{g}{U_0 \cos \beta}}^{\infty} \left(1 - \frac{2U_0 \cos \beta}{g} \omega_3 \right) \omega_3 e^{k_3[z + i(x \cos \beta + y \sin \beta + U_0 t \cos \beta)]} e^{-i \omega_3 t} d\omega_3 \right\}$$

$$\zeta^{(\omega_1)}(t) = \frac{1}{\pi} \operatorname{Re} \left\{ \int_0^{\frac{g}{2U_0 \cos \beta}} \bar{\zeta}(\omega_1) e^{i \omega_1 (1 - \frac{\omega_1 U_0 \cos \beta}{g}) t} d\omega_1 \right\}$$

$$\zeta^{(\omega_2)}(t) = -\frac{1}{\pi} \operatorname{Re} \left\{ \int_{\frac{g}{2U_0 \cos \beta}}^{\frac{g}{U_0 \cos \beta}} \bar{\zeta}(\omega_2) e^{i \omega_2 (1 - \frac{\omega_2 U_0 \cos \beta}{g}) t} d\omega_2 \right\} \quad (34)$$

$$\zeta^{(\omega_3)}(t) = -\frac{1}{\pi} \operatorname{Re} \left\{ \int_{\frac{g}{U_0 \cos \beta}}^{\infty} \bar{\zeta}(\omega_3) e^{i \omega_3 (1 - \frac{\omega_3 U_0 \cos \beta}{g}) t} d\omega_3 \right\}$$

ω_2 、 ω_3 范围对应的脉冲函数和波高表达式前面都有负号，和 Korsmeyer 和 Bingham^[13]一致，脉冲函数和波高相乘时相互抵消，后续 ω_2 、 ω_3 范围对应的脉冲函数和波高表达式负号都去掉，和 Osborne^[12]一致。三个入射波频率范围对应的入射波压力和绕射势脉冲函数可写成如下表达式：

$$\hat{p}^{(\omega_1)}(P, t) = \frac{\rho g}{\pi} \operatorname{Re} \left\{ I_0^{(\omega_1)}(\alpha, b) - \frac{2U_0 \cos \beta}{g} I_1^{(\omega_1)}(\alpha, b) \right\}$$

$$\hat{p}^{(\omega_2)}(P, t) = \frac{\rho g}{\pi} \operatorname{Re} \left\{ I_0^{(\omega_2)}(\alpha, b) - \frac{2U_0 \cos \beta}{g} I_1^{(\omega_2)}(\alpha, b) \right\} \quad (35)$$

$$\hat{p}^{(\omega_3)}(P, t) = \frac{\rho g}{\pi} \operatorname{Re} \left\{ I_0^{(\omega_3)}(\alpha, b) - \frac{2U_0 \cos \beta}{g} I_1^{(\omega_3)}(\alpha, b) \right\}$$

$$\hat{K}^{(\omega_1)}(P, t) = \frac{1}{\pi} \operatorname{Re} \left\{ \begin{bmatrix} \hat{i} \cos \beta \\ \hat{j} \cos \beta \\ \hat{k} i \end{bmatrix} \left(I_1^{(\omega_1)}(\alpha, b) - \frac{2U_0 \cos \beta}{g} I_2^{(\omega_1)}(\alpha, b) \right) \right\}$$

$$\hat{K}^{(\omega_2)}(P, t) = \frac{1}{\pi} \operatorname{Re} \left\{ \begin{bmatrix} \hat{i} \cos \beta \\ \hat{j} \cos \beta \\ \hat{k} i \end{bmatrix} \left(I_1^{(\omega_2)}(\alpha, b) - \frac{2U_0 \cos \beta}{g} I_2^{(\omega_2)}(\alpha, b) \right) \right\} \quad (36)$$

$$\hat{K}^{(\omega_3)}(P, t) = \frac{1}{\pi} \operatorname{Re} \left\{ \begin{bmatrix} \hat{i} \cos \beta \\ \hat{j} \cos \beta \\ \hat{k} i \end{bmatrix} \left(I_1^{(\omega_3)}(\alpha, b) - \frac{2U_0 \cos \beta}{g} I_2^{(\omega_3)}(\alpha, b) \right) \right\}$$

通过式(35)~(36)可以看出，分别求出三个入射波频率范围的 $I_0(\alpha, b)$ 、 $I_1(\alpha, b)$ 、 $I_2(\alpha, b)$ 后，即可求出随浪/尾斜浪中绕射速度势和入射波压力脉冲函数表达式。根据式(19)~(22)，三个入射波频率范围的 $I_0(\alpha, b)$ 、 $I_1(\alpha, b)$ 、 $I_2(\alpha, b)$ 求解方法如下。

$$I_0^{(\omega_1)} = \int_0^{\frac{g}{2U_0 \cos \beta}} e^{-(\alpha x^2 + 2bx)} dx = \frac{1}{2} \sqrt{\frac{\pi}{\alpha}} \left[w\left(\frac{ib}{\sqrt{\alpha}}\right) - e^{-\left(\frac{ga}{4U_0^2 \cos^2 \beta} + \frac{gb}{U_0 \cos \beta}\right)} w\left(\frac{ig\sqrt{\alpha}}{2U_0 \cos \beta} + \frac{ib}{\sqrt{\alpha}}\right) \right] \quad (37)$$

$$I_1^{(\omega_1)} = \int_0^{\frac{g}{2U_0 \cos \beta}} x e^{-(\alpha x^2 + 2bx)} dx = \frac{-b}{\alpha} I_0^{(\omega_1)} - \frac{1}{2\alpha} e^{-\left(\frac{g^2 \alpha}{4U_0^2 \cos^2 \beta} + \frac{gb}{U_0 \cos \beta}\right)} + \frac{1}{2\alpha} \quad (38)$$

$$I_2^{(\omega_1)} = \int_0^{\frac{g}{2U_0 \cos \beta}} x^2 e^{-(\alpha x^2 + 2bx)} dx = \frac{1}{2\alpha} I_0^{(\omega_1)} - \frac{b}{\alpha} I_1^{(\omega_1)} - \frac{g}{4\alpha U_0 \cos \beta} e^{-\left(\frac{g^2 \alpha}{4U_0^2 \cos^2 \beta} + \frac{gb}{U_0 \cos \beta}\right)} \quad (39)$$

$$I_0^{(\omega_2)} = \int_{\frac{g}{2U_0 \cos \beta}}^{\frac{g}{U_0 \cos \beta}} e^{-(\alpha x^2 + 2bx)} dx = \frac{1}{2} \sqrt{\frac{\pi}{\alpha}} \left[e^{-\left(\frac{ga}{4U_0^2 \cos^2 \beta} + \frac{gb}{U_0 \cos \beta}\right)} w\left(\frac{ig\sqrt{\alpha}}{2U_0 \cos \beta} + \frac{ib}{\sqrt{\alpha}}\right) - e^{-\left(\frac{ga}{U_0^2 \cos^2 \beta} + \frac{2gb}{U_0 \cos \beta}\right)} w\left(\frac{ig\sqrt{\alpha}}{U_0 \cos \beta} + \frac{ib}{\sqrt{\alpha}}\right) \right] \quad (40)$$

$$I_1^{(\omega_2)} = \int_{\frac{g}{2U_0 \cos \beta}}^{\frac{g}{U_0 \cos \beta}} x e^{-(\alpha x^2 + 2bx)} dx = \frac{-b}{\alpha} I_0^{(\omega_2)} - \frac{1}{2\alpha} \left(e^{-\left(\frac{g^2 \alpha}{U_0^2 \cos^2 \beta} + \frac{2gb}{U_0 \cos \beta}\right)} - e^{-\left(\frac{g^2 \alpha}{4U_0^2 \cos^2 \beta} + \frac{gb}{U_0 \cos \beta}\right)} \right) \quad (41)$$

$$I_2^{(\omega_2)} = \int_{\frac{g}{2U_0 \cos \beta}}^{\frac{g}{U_0 \cos \beta}} x^2 e^{-(\alpha x^2 + 2bx)} dx = \frac{1}{2\alpha} I_0^{(\omega_2)} - \frac{b}{\alpha} I_1^{(\omega_2)} - \frac{g}{2\alpha U_0 \cos \beta} e^{-\left(\frac{g^2 \alpha}{U_0^2 \cos^2 \beta} + \frac{2gb}{U_0 \cos \beta}\right)} + \frac{g}{4\alpha U_0 \cos \beta} e^{-\left(\frac{g^2 \alpha}{4U_0^2 \cos^2 \beta} + \frac{gb}{U_0 \cos \beta}\right)} \quad (42)$$

$$I_0^{(\omega_3)} = \int_0^{\frac{g}{2U_0 \cos \beta}} e^{-(\alpha x^2 + 2bx)} dx = \frac{1}{2} \sqrt{\frac{\pi}{\alpha}} \left[w\left(\frac{ib}{\sqrt{\alpha}}\right) - e^{-\left(\frac{ga}{4U_0^2 \cos^2 \beta} + \frac{gb}{U_0 \cos \beta}\right)} w\left(\frac{ig\sqrt{\alpha}}{2U_0 \cos \beta} + \frac{ib}{\sqrt{\alpha}}\right) \right] \quad (43)$$

$$I_1^{(\omega_3)} = \int_{\frac{g}{2U_0 \cos \beta}}^{\infty} x e^{-(\alpha x^2 + 2bx)} dx = \frac{-b}{\alpha} I_0^{(\omega_3)} + \frac{1}{2\alpha} e^{-\left(\frac{g^2 \alpha}{U_0^2 \cos^2 \beta} + \frac{2gb}{U_0 \cos \beta}\right)} \quad (44)$$

$$I_2^{(\omega_3)} = \int_{\frac{g}{2U_0 \cos \beta}}^{\infty} x^2 e^{-(\alpha x^2 + 2bx)} dx = \frac{1}{2\alpha} I_0^{(\omega_3)} - \frac{b}{\alpha} I_1^{(\omega_3)} + \frac{g}{2\alpha U_0 \cos \beta} e^{-\left(\frac{g^2 \alpha}{U_0^2 \cos^2 \beta} + \frac{2gb}{U_0 \cos \beta}\right)} \quad (45)$$

1.6 复数误差函数求解方法

1.4节和1.5节中复数误差函数 $w(z)$ 中 z 已给出具体表达式, 求出 $w(z)$ 或 $w(x+iy)$ 的实部和虚部, 即可求出 $I_0(\alpha, b)$, 进而求出 $I_1(\alpha, b)$ 、 $I_2(\alpha, b)$ 和脉冲函数。

当 $|\operatorname{Re}(z)| < 5.33$, $|\operatorname{Im}(z)| < 4.29$ 时, Gautschi^[30-31] 给出了计算 $w(z)$ 的实部和虚部代码。当 z 不在这个范围时, 采用 Gauss-Hermite 积分方法求解 $w(z)$ 的实部和虚部。根据文献[31]和[32], 复数误差函数 $w(z)$ 可写成公式:

$$w(z) = \begin{cases} K[\operatorname{Re}(z), \operatorname{Im}(z)] + iL[\operatorname{Re}(z), \operatorname{Im}(z)] & y \geq 0 \\ K[\operatorname{Re}(z), \operatorname{Im}(z)] + iL[\operatorname{Re}(z), \operatorname{Im}(z)] + \operatorname{Re}(2e^{-z^2}) + i\operatorname{Im}(2e^{-z^2}) & y < 0 \end{cases} \quad (46)$$

$$K[\operatorname{Re}(z), \operatorname{Im}(z)] = \frac{\operatorname{Im}(z)}{\pi} \int_{-\infty}^{\infty} \frac{e^{-t^2}}{(\operatorname{Re}(z) - t)^2 + \operatorname{Im}(z)^2} dt \approx \frac{\operatorname{Im}(z)}{\pi} \sum_{i=1}^n w_i \frac{1}{(\operatorname{Re}(z) - t_i)^2 + \operatorname{Im}(z)^2} \quad (47)$$

$$L[\operatorname{Re}(z), \operatorname{Im}(z)] = \frac{1}{\pi} \int_{-\infty}^{\infty} \frac{(\operatorname{Re}(z) - t)e^{-t^2}}{(\operatorname{Re}(z) - t)^2 + \operatorname{Im}(z)^2} dt \approx \frac{1}{\pi} \sum_{i=1}^n w_i \frac{(\operatorname{Re}(z) - t_i)}{(\operatorname{Re}(z) - t_i)^2 + \operatorname{Im}(z)^2}$$

$$\operatorname{Re}[2e^{-z^2}] = \operatorname{Re}\left[2e^{-[\operatorname{Re}(z) + i\operatorname{Im}(z)]^2}\right] = 2e^{-\operatorname{Re}(z)^2 + \operatorname{Im}(z)^2} \cos[2\operatorname{Re}(z)\operatorname{Im}(z)] \quad (48)$$

$$\operatorname{Im}[2e^{-z^2}] = \operatorname{Im}\left[2e^{-[\operatorname{Re}(z) + i\operatorname{Im}(z)]^2}\right] = 2e^{-\operatorname{Re}(z)^2 + \operatorname{Im}(z)^2} \sin[2\operatorname{Re}(z)\operatorname{Im}(z)]$$

公式(47)用到 Gauss-Hermite 积分方法, t_i 为高斯节点, w_i 为权重。当 n 取到 10 时, 高斯点和权重值如下:

$$\begin{aligned} t_1 &= -3.4361591188377376, & w_1 &= 7.6404328552326206E-6; & t_2 &= -2.5327316742327898, & w_2 &= 0.0013436457467812 \\ t_3 &= -1.7566836492998818, & w_3 &= 0.0338743944554811; & t_4 &= -1.0366108297895137, & w_4 &= 0.2401386110823147 \\ t_5 &= -0.3429013272237046, & w_5 &= 0.6108626337353258; & t_6 &= 0.3429013272237046, & w_6 &= 0.6108626337353258 \\ t_7 &= 1.0366108297895137, & w_7 &= 0.2401386110823147; & t_8 &= 1.7566836492998818, & w_8 &= 0.0338743944554811 \\ t_9 &= 2.5327316742327898, & w_9 &= 0.0013436457467812; & t_{10} &= 3.4361591188377376, & w_{10} &= 7.6404328552326206E-6 \end{aligned} \quad (49)$$

2 数值计算方法验证

2.1 顶浪中垂荡纵摇脉冲函数和波浪力的收敛性计算及验证

图2和图3分别给出了Wigley I船^[33]在顶浪中零航速时无量纲化垂荡、纵摇的FK力和绕射力脉冲响应函数,图中图标“Present”表示本文计算结果,“King 1987”表示文献King^[7]的结果,后续图中表示方法类似。本文计算结果和King^[7]的计算结果吻合。图4给出了Wigley I船在顶浪中 $F_n=0.3$ 时无量纲化垂荡、纵摇的FK力+绕射力脉冲响应函数,本文计算结果和Osborne^[12]的计算结果吻合。从图2~4的结果可以看出,顶浪中FK力和绕射力脉冲响应函数比较稳定,能在较短时间内收敛。图5和图6给出了Wigley I船在顶浪中 $F_n=0.3$ 时不同波长时垂荡、纵摇的FK力+绕射力振幅和相位,本文计算结果和Journee^[33]的试验结果、Bingham^[11]的计算结果基本一致。

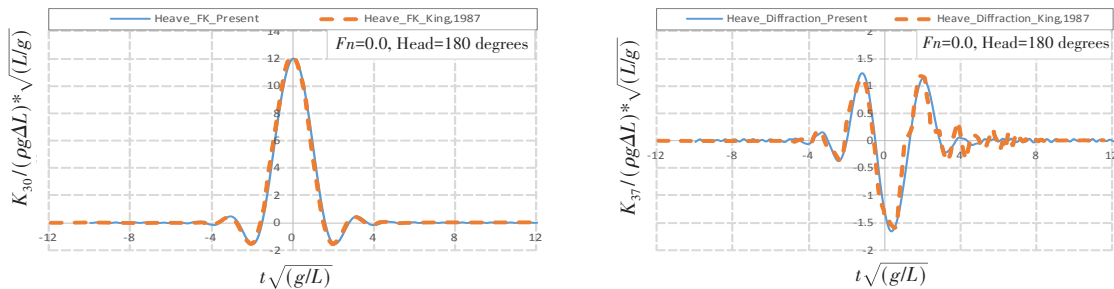


图2 Wigley I船顶浪中零航速时无量纲化垂荡FK力和绕射力脉冲响应函数
Fig.2 Nondimensional FK force and diffraction force impulse response functions during heaving motion for Wigley I at $F_n=0.0$ in head seas

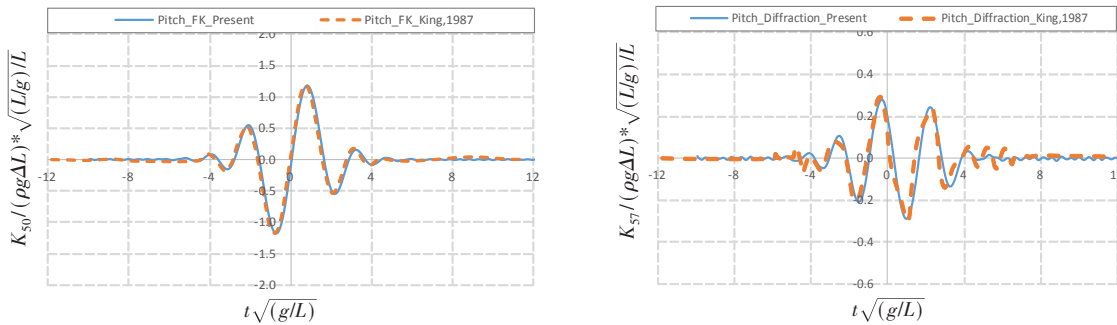


图3 Wigley I船顶浪中零航速时无量纲化纵摇FK力和绕射力脉冲响应函数
Fig.3 Nondimensional FK force and diffraction impulse response functions during pitching motion for Wigley I at $F_n=0.0$ in head seas

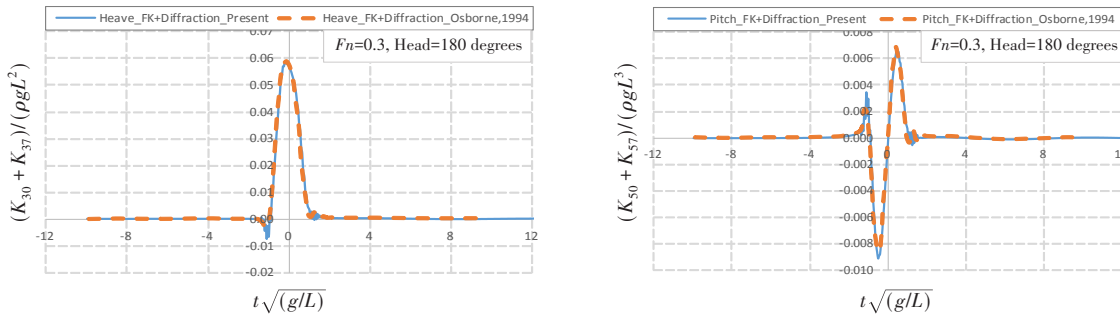


图4 Wigley I船顶浪中 $F_n=0.3$ 时无量纲化垂荡、纵摇的FK力和绕射力脉冲响应函数
Fig.4 Nondimensional FK and diffraction impulse response function during heaving and pitching motion for Wigley I at $F_n=0.3$ in head seas

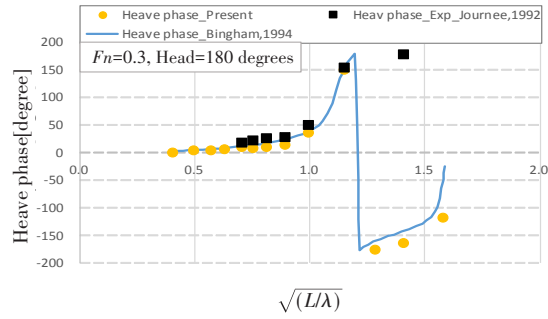
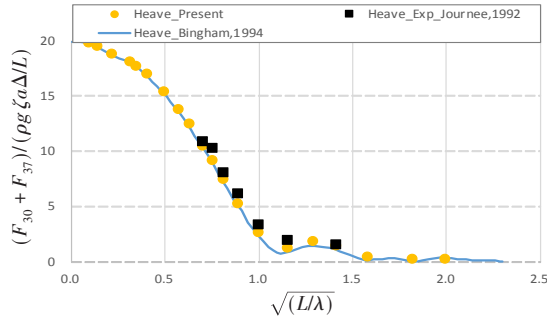


图5 Wigley I船顶浪中 $F_n=0.3$ 时无量纲化垂荡FK力和绕射力的振幅和相位

Fig.5 Nondimensional FK and diffraction force and its phase during heaving motion for Wigley I at $F_n=0.3$ in head seas

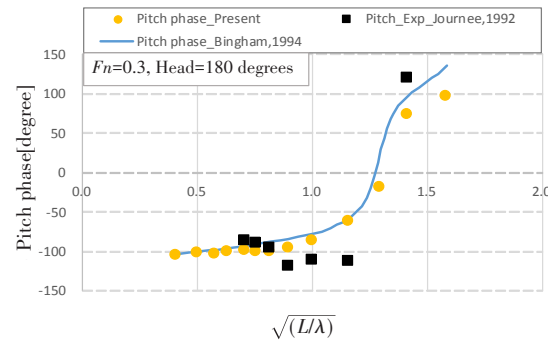
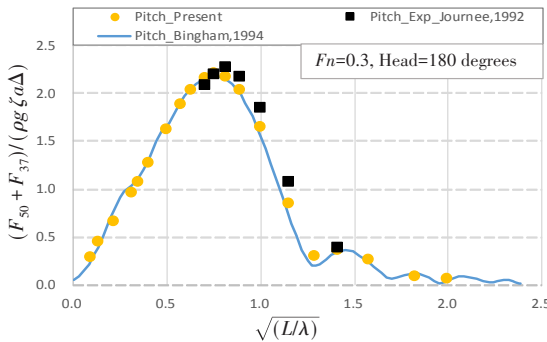


图6 Wigley I船顶浪中 $F_n=0.3$ 时无量纲化纵摇FK力和绕射力的振幅和相位

Fig.6 Nondimensional FK and diffraction force and its phase during pitching motion for Wigley I at $F_n=0.3$ in head seas

2.2 随浪中垂荡纵摇脉冲函数和波浪力的收敛性计算及验证

图7~9分别给出了Wigley I船在随浪中 $F_n=0.3$ 时三个入射波频率范围的无量纲化垂荡、纵摇的FK力+绕射力脉冲响应函数,本文计算结果和Osborne^[12]的计算结果吻合。在 ω_1 和 ω_2 两个低频入射波频率范围内,如图7和图8所示,FK力+绕射力脉冲响应函数能够快速收敛,但收敛时间比顶浪状态下的长。在 ω_3 高频入射波频率范围内,如图9所示,FK力+绕射力脉冲响应函数收敛性较差。在 ω_3 频率范围内,本文计算采用的网格数为 $28 \times 6 \times 2$,但入射波频率高,波长较短。网格数和波浪高频影响,后续需要进一步分析。图10给出了Wigley I船在随浪中 $F_n=0.3$ 时三个入射波频率范围的无量纲化垂荡、纵摇的FK力+绕射力振幅,本文计算结果和Osborne^[12]的计算结果整体吻合较好,在 ω_3 频率范围存在差异,原因是该范围内 ω_3 频率范围内收敛性较差。图11和图12给出了Wigley I船在随浪中 $F_n=0.3$ 时不同波长时垂荡、纵摇的FK力+绕射力振幅和相位,本文计算结果和Osborne^[12]的计算结果吻合较好。

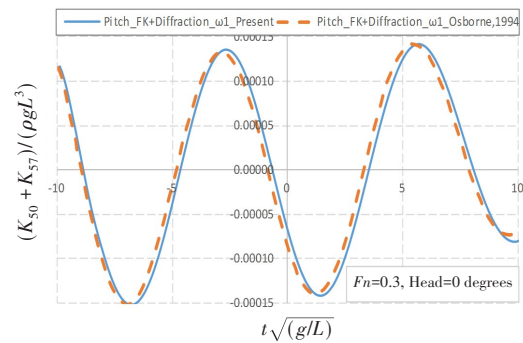
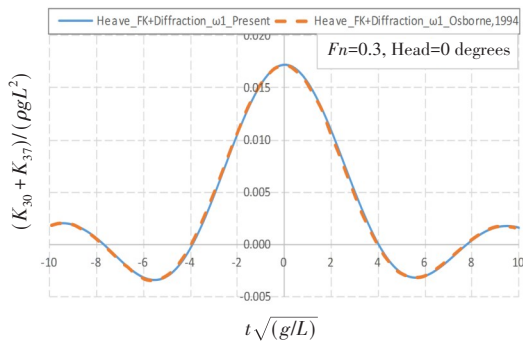


图7 Wigley I船随浪中 $F_n=0.3$ 时无量纲化垂荡、纵摇的FK力和绕射力脉冲响应函数(ω_1)

Fig.7 Nondimensional FK and diffraction force impulse response function in heaving and pitching motion for Wigley I at $F_n=0.3$ in following seas (ω_1)

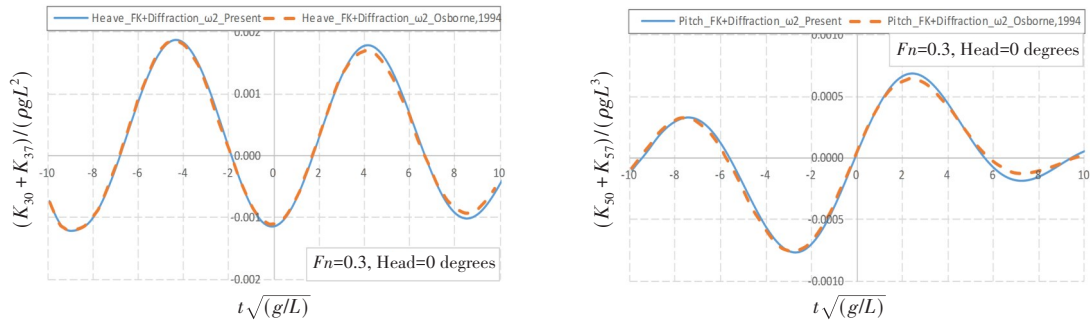


图8 Wigley I船随浪中 $F_n=0.3$ 时无量纲化垂荡、纵摇的FK力和绕射力脉冲响应函数(ω_2)

Fig.8 Nondimensional FK and diffraction force impulse response function in heaving and pitching motion for Wigley I at $F_n=0.3$ in following seas (ω_2)

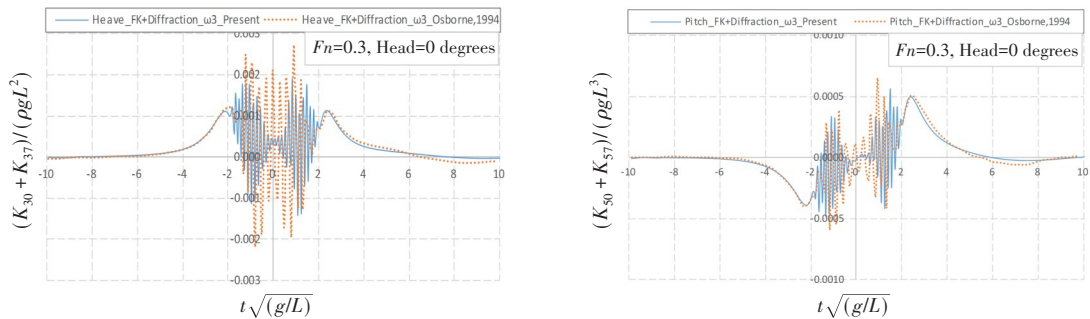


图9 Wigley I船随浪中 $F_n=0.3$ 时无量纲化垂荡、纵摇的FK力和绕射力脉冲响应函数(ω_3)

Fig.9 Nondimensional FK and diffraction force impulse response function in heaving and pitching motion for Wigley I at $F_n=0.3$ in following seas (ω_3)

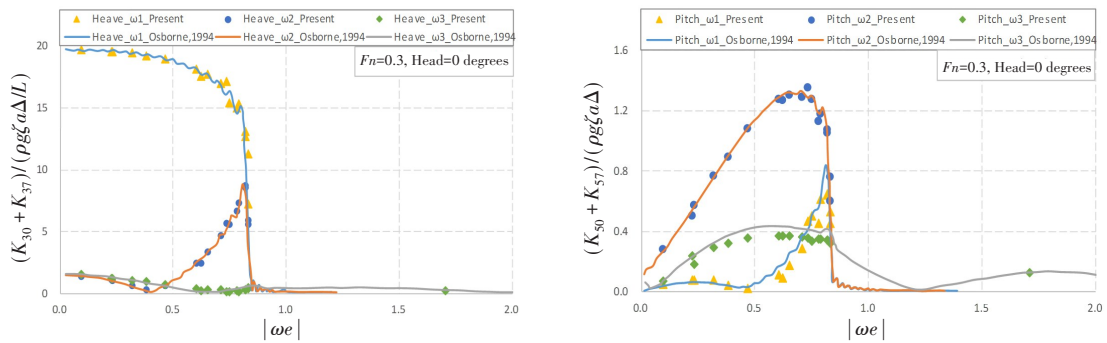


图10 Wigley I船随浪中 $F_n=0.3$ 时不同入射波频率的无量纲化垂荡和纵摇FK力和绕射力的振幅

Fig.10 Nondimensional FK and diffraction force in heaving and pitching motion for Wigley I at $F_n=0.3$ in following seas with different wave frequencies

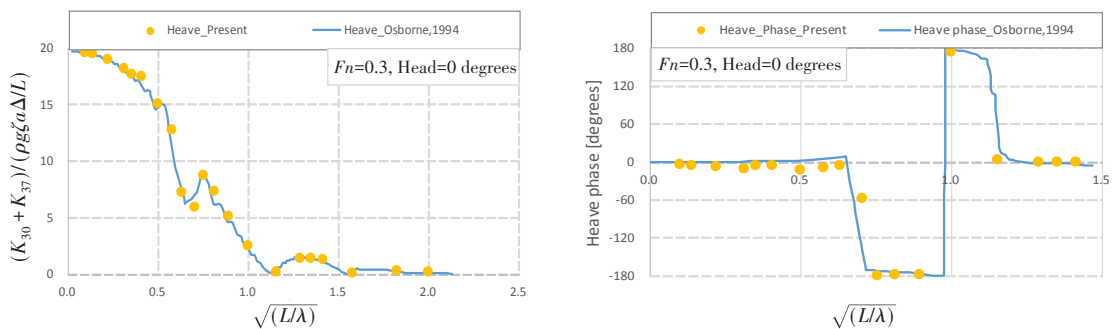


图11 Wigley I船随浪中 $F_n=0.3$ 时无量纲化垂荡FK力和绕射力的振幅和相位

Fig.11 Nondimensional FK and diffraction force and its phase in heaving motion for Wigley I at $F_n=0.3$ in following seas

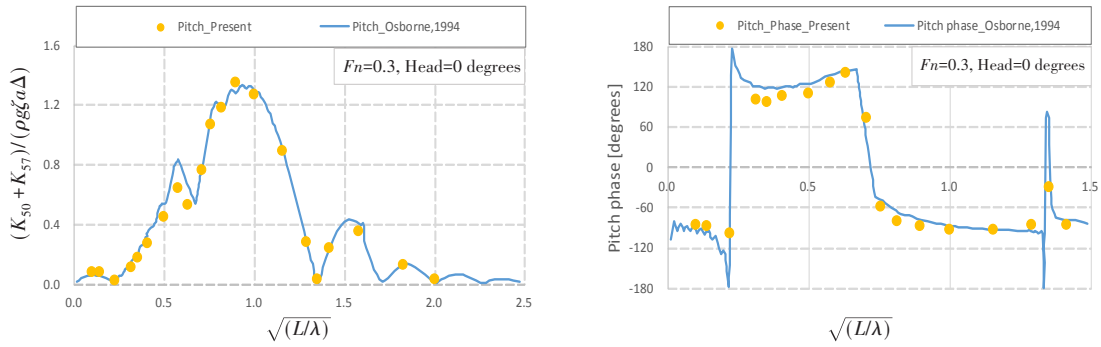


图 12 Wigley I 船随浪中 $F_n=0.3$ 时无量纲化纵摇 FK 力和绕射力的振幅和相位

Fig.12 Nondimensional FK and diffraction force and its phase in pitching motion for Wigley I at $F_n=0.3$ in following seas

3 结 论

本文以美国密歇根大学 Beck 团队的三维时域面元法为参照,推导出可直接用于程序开发的全浪向绕射力数学展开表达式,通过 Wigley I 船型,验证了本文方法的时域绕射力的收敛性,得出如下结论:

- (1) 在随浪高频入射波频率范围内绕射力脉冲函数收敛性较差,在其他两个入射波频率范围内,绕射力脉冲函数收敛性较快,但收敛时间长于顶浪的情况;
- (2) 本文采用的三维时域自由面格林函数法和全浪向绕射力数学表达式,可以可靠地计算出顶浪和随浪中的三维时域绕射力脉冲函数和绕射力;
- (3) 本文推导给出了可直接用于程序开发的全浪向绕射力数学展开表达式和求解过程,有助于从事此方面研究的人员进行编程应用,实用性强。

本文方法和代码可用于船舶工业 CAE 软件势流求解器,并可用于波浪中船舶非线性失稳运动预报。

参 考 文 献:

[1] 鲁 江,张 楠,张新曙,等. 船舶有航速时三维时域格林函数计算方法研究[J]. 船舶力学, 2024, 28(1): 20-35.
 Lu Jiang, Zhang Nan, Zhang Xinshu, et al. Study on the convergence of the radiation force using three-dimensional time-domain Green function method[J]. Journal of Ship Mechanics, 2024, 28(1): 20-35. (in Chinese)

[2] Finkelstein A B. The initial value problem for transient water waves[J]. Communications on Pure and Applied Mathematics, 1957, 10(4): 511-522.

[3] Cummins W E. The impulse response function and ship motions[J]. Schiffstechnik, 1962, 9: 101-109.

[4] Ogilvie T F. Recent progress toward the understanding and prediction of ship motions[C]//Proceeding of 5th Symposium on Naval Hydrodynamics, ONR, Washington, D.C., 1964: 3-128.

[5] Wehausen J V, Laitone E V. Surface waves. Handbuch der physic[M]. Berlin: Springer-Verlag, 1960: 446-778.

[6] Liapis S J. Time-domain analysis of ship motions[D]. The University of Michigan, 1986.

[7] King B. Time-domain analysis of wave exciting forces on ships and bodies[D]. The University of Michigan, 1987.

[8] Magee A R. Large-amplitude ship motions in the time domain[D]. Ann Arbor: University of Michigan, 1991.

[9] Newman J N. The evaluation of free surface Green functions[C]//4th International Conference on Numerical Ship Hydrodynamics, Washington D C, 1985.

- [10] Newman J N. The approximation of free surface Green functions[C]//Proceeding of the Fritz Ursell Retirement Meeting, Manchester, England, 1990: 107-135
- [11] Bingham H B. Simulating ship motions in the time domain[D]. Cambridge: Massachusetts Institute of Technology, 1994.
- [12] Osborne G E. The forward speed diffraction problem in following seas[D]. Cambridge: Massachusetts Institute of Technology, 1994.
- [13] Korsmeyer F T, Bingham H B. The forward speed diffraction problem[J]. *Journal of Ship Research*, 1998, 42(2): 99-112.
- [14] Lin W M, Yue D K P. Numerical solution for large-amplitude ship motions in time domain[C]//18th Symposium on Naval Hydrodynamics, Ann Arbor, Michigan, 1990.
- [15] Lin W M, Zhang S, Weems K, et al. A mixed source formulation for nonlinear ship-motion and wave-load simulations[C]//7th International Conference on Numerical Ship Hydrodynamics, Paris, France, 1999.
- [16] Shin Y S, Belenky V L, Lin W M, et al. Nonlinear time domain simulation technology for seakeeping and wave-load analysis for modern ship design[M]. ABS Technology Papers, 2003.
- [17] Zhou Zhengquan, Gu Maoxiang. A numerical research of non-linear body-wave interactions[C]//18th Symposium on Naval Hydrodynamics, Ann Arbor, Michigan, 1990: 103-118.
- [18] 黄德波. 时域 Green 函数及其导数的数值计算[J]. *中国造船*, 1992, 119(4): 16-25.
Huang Debo. Approximation of time-domain free surface function and its spatial derivatives[J]. *Shipbuilding of China*, 1992, 119 (4): 16-25. (in Chinese)
- [19] 周正全, 张亮, 戴遗山. 船舶在波浪中航行时绕射问题的线性时域解[J]. *中国造船*, 1993, 3(122): 1-25.
Zhou Zhengquan, Zhang Liang, Dai Yishan. Time-domain analysis of wave diffraction for ship motions with forward speed [J]. *Shipbuilding of China*, 1993, 3 (122): 1-25. (in Chinese)
- [20] 王大云. 三维船舶水弹性力学的线性时域分析方法[D]. 无锡: 中国船舶科学研究中心, 1996. (in Chinese)
Wang Dayun. Three-dimensional hydroelastic analysis of ships in time domain[D]. Wuxi: China Ship Scientific Research Center, 1996. (in Chinese)
- [21] Clement A H. An ordinary differential equation for the Green function of time-domain free-surface hydrodynamics[J]. *Journal of Engineering Mathematics*, 1998, 33: 201-217.
- [22] Duan W Y, Dai Y S. New derivation of ordinary different equation for time-domain free-surface Green Functions[J]. *China Ocean Engineering*, 2001, 15(4): 499-507.
- [23] 申亮, 朱仁传, 缪国平, 等. 深水时域格林函数的实用数值计算[J]. *水动力学研究与进展(A辑)*, 2007, 22(3): 380-386.
Shen Liang, Zhu Renchuan, Miao Guoping, et al. A practical numerical method for deep water time-domain Green function [J]. *Journal of Hydrodynamics*, 2007, 22(3): 380-386. (in Chinese)
- [24] 杨鹏. 船舶三维时域非线性水弹性响应研究[D]. 无锡: 中国船舶科学研究中心, 2016.
Yang Peng. 3D nonlinear hydroelastic response study of ships in time domain[D]. Wuxi: China Ship Scientific Research Center, 2016. (in Chinese)
- [25] 卜淑霞, 鲁江, 顾民, 等. 基于三维时域混合源法的顶浪不规则波参数横摇研究[J]. *船舶力学*, 2018, 22(8): 926-934.
Bu Shuxia, Lu Jiang, Gu Min, et al. A study on parametric roll in irregular head waves by a 3D time domain hybrid panel method[J]. *Journal of Ship Mechanics*, 2018, 22(8): 926-934. (in Chinese)
- [26] 储纪龙, 顾民, 鲁江, 等. 规则波中参数横摇直接稳性评估方法研究[J]. *水动力学研究与进展*, 2019, 34(1): 39-44.
Chu Jilong, Gu Min, Lu Jiang, et al. Study on the direct stability assessment method of parametric roll in regular waves[J]. *Journal of Hydrodynamics*, 2019, 34(1): 39-44. (in Chinese)
- [27] Chen J K, Duan W Y, Ma S, Li J D. Time domain TEBEM method of ship motion in waves with forward speed by using impulse response function formulation[J]. *Ocean Engineering*, 2021, 227, 108617.
- [28] Hess J L, Simith A M O. Calculation of nonlifting potential flow about arbitrary three-dimensional bodies[J]. *Journal of Ship Research*, 1964, 8(2): 22-24.
- [29] Abramowitz M, Stegun I A. Handbook of mathematical function[M]. Washington D C: National Bureau of Standards, 1964.

-
- [30] Gautschi W. The complex error function[M]. Collected Algorithms from Communications of the Association for Computing Machinery, Algorithm 363, 1969.
- [31] Gautschi W. Efficient computation of the complex error function[J]. SIAM Journal on Numerical Analysis, 1970, 7(1): 187–198.
- [32] Abrarov S M, Quine B M. A rational approximation for efficient computation of the voigt function in quantitative spectroscopy[J]. Journal of Mathematics Research, 2015, 7(2): 163–174.
- [33] Journée J M J. Experiments and calculations on 4 wigley hull forms in head waves[R]. Delft University of Technology Report, 1992.